Multiview Cloud-Top Height and Wind Retrieval with Photogrammetric Methods: Application to *Meteosat-8* HRV Observations

GABRIELA SEIZ

Institute of Geodesy and Photogrammetry, Swiss Federal Institute of Technology ETH, Zürich, Switzerland

STEPHEN TJEMKES AND PHILIP WATTS

European Organisation for the Exploitation of Meteorological Satellites, Darmstadt, Germany

ABSTRACT

The European Organisation for the Exploitation of Meteorological Satellites (EUMETSAT) currently operates three geostationary satellites: *Meteosat-5*, *Meteosat-7*, and *Meteosat-8*. Observations by *Meteosat-5* can be combined with observations from either *Meteosat-7* or *Meteosat-8* to allow geostationary stereo height retrievals within the overlap area over the Indian Ocean and east Africa. This paper aims to demonstrate the capabilities of the geostationary stereophotogrammetric cloud-top height retrieval—in particular, with the new high-resolution visible channel (HRV) of *Meteosat-8*. Conceived as a proof-of-concept study, the retrieval was limited to four distinct cloud areas in northeast Africa. The effects of the geolocation, spatial resolution, satellite position, and acquisition time on the cloud-top height accuracy were studied. It is demonstrated that the matching accuracy is sensitive to the acquisition-time difference and spatial resolution. As a result, there is only a marginal benefit from the good spatial resolution offered by the *Meteosat-8* HRV channel because of the low spatial resolution of *Meteosat-5* and the poor time synchronization between the observations of the two satellites. On the contrary, the good time synchronization between *Meteosat-5* and *Meteosat-7* observations offsets the errors in the height assignment resulting from the relatively coarse spatial resolution, if the geolocation accuracy is locally enhanced with additional landmarks from higher-resolution images. With the geolocation correction and the newly implemented time information in the *Meteosat-5* and *-7* header information, the stereo cloud-top height assignment for the *Meteosat-5/-7* and *Meteosat-5/-8* HRV combination resulted in about the same accuracy of approximately ±1 km. For the *Meteosat-5/-8* HRV combination, the time differences of up to 7.5 min preclude higher accuracy. To validate the cloud-top heights, observations by the Multiangle Imaging Spectroradiometer (MISR) and Moderate Resolution Imaging Spectroradiometer (MODIS) were used.

1. Introduction

Satellite-based stereoscopy of clouds has a long tradition in meteorology, from both geostationary and polar-orbiting sensors. In this paper, we focus on the use of geostationary satellites for the stereophotogrammetric determination of cloud-top height (CTH), as previously described in, for example, Hasler (1981), Fujita (1982), Wylie et al. (1998), and Campbell and Holmlund (2000, 2004). Stereo measurements have the advantage that they depend only on basic geometric relationships of observations of cloud features from at least two different viewing angles. Other CTH estimation methods are dependent on the knowledge of additional cloud/atmosphere parameters like cloud emissivity, ambient temperature, or lapse rate. Even though these methods are dependent on auxiliary data, the accuracy of these methods has been established by various authors and has been estimated to be between 80 and 100 hPa, depending on the cloud type (Nieman et al. 1993; Naud et al. 2005a; Preusker et al. 2005).

The European Organisation for the Exploitation of Meteorological Satellites (EUMETSAT) currently operates instruments on three geostationary satellites: *Meteosat-5*, *-7*, and *-8*, located at 63°E, 0°, and 3.3°W,

Corresponding author address: Dr. Gabriela Seiz, Swiss Federal Office of Meteorology and Climatology MeteoSwiss, Kraehbuehlstr. 58, Zürich CH-8044, Switzerland.
E-mail: gabriela.seiz@meteoswiss.ch

respectively.[1] Observations by *Meteosat-5* can be combined with observations from either *Meteosat-7* or *Meteosat-8* to allow geostationary stereo height retrievals within the overlap area over the Indian Ocean and east Africa.

The infrared (IR) channels of the *Meteosat-5/-7* combination have been analyzed by Campbell and Holmlund (2000, 2004). They were able to derive CTH of cloud systems with an estimated accuracy of approximately 2 km, which would be comparable to the accuracy of the traditional methods. However, their error estimation only took into account the matching error and no further errors from geolocation, observation time, and so on. No comparison with independent data was included in their study to confirm the theoretical error estimates.

The observations by the new Spinning Enhanced Visible and Infrared Radiometer Instrument (SEVIRI) on board *Meteosat-8* can be used in combination with the *Meteosat-5* observations to determine CTH using stereophotogrammetric methods. Of particular interest is the use of the so-called high-resolution visible (HRV) channel, which has a spatial resolution at the subsatellite point (SSP) of about 1.0 km. This higher resolution should translate into more accurate stereo cloud-top heights. The accuracy of the derived CTH depends not only on the spatial resolution of the adopted observations, but also critically on the accurate matching of the observed cloud features. The matching accuracy is reduced by time differences between the observations. The larger the time difference is, the more difficult is the matching, on average, because of changes in the cloud structures. There unfortunately is a significant time difference (of up to ±7.5 min) between the *Meteosat-5* and *Meteosat*-8 HRV image resulting from the different scan period (i.e., 30 and 15 min, respectively). By contrast, the time difference between *Meteosat-5* and *Meteosat-7* observations is small (on average less than ±10 s, except for regions toward the image borders). Hence, it is not obvious that by replacing *Meteosat-7* with *Meteosat-8* HRV observations, the CTH accuracy would increase as expected by Campbell and Holmlund (2004).

This paper extends the multiview cloud-top height

---

[1] Note that, with the installation of *Meteosat-6* as a rapid-scanning geostationary satellite for the Mesoscale Alpine Program in autumn of 1999 and operationally since September of 2001, a potential additional Meteosat stereo configuration is available with a large overlap area over Europe. This stereo configuration of 10° longitudinal separation (i.e., *Meteosat-6* at 10°E) unfortunately cannot be used for quantitative stereo analysis, because for acceptable stereo CTH accuracies of ±1 km or better a longitude separation of at least 50° is required.

and motion retrievals described in Seiz and Baltsavias (2000) and Seiz et al. (2001, 2003) to geostationary stereo height and motion retrieval, with special focus on the new *Meteosat-8* HRV/*Meteosat-5* combination. Thereby, the main objective is to document—as a proof-of-concept study—the accuracy and limitations of the stereo height assignment using the *Meteosat-8* HRV and the visible channels on either *Meteosat-5* or *-7*. For the analysis, four different clouds in the vicinity of coastlines were selected. These coastlines were used as landmarks for an accurate absolute geolocation of the Meteosat images. Coincident observations by the Multiangle Imaging Spectroradiometer (MISR) were used to provide independent estimation of the cloud-top height. The high spatial resolution as well as the good geolocation of the MISR views enabled an accurate estimation of the CTH for these clouds. Further independent estimates were obtained from the Moderate-Resolution Imaging Spectroradiometer (MODIS) operational product. The operational MISR and MODIS CTH products have been extensively compared and validated by Naud et al. (2005b). Because this study was conceived as a proof-of-concept study for the different important elements of geostationary stereo CTH retrieval, no attempt was made to evaluate the method systematically with a large number of scenes, stratified by cloud type, acquisition time, and so on. This further step should be done as soon as a stereo configuration of two synchronized (or quasi synchronized within a few seconds) geostationary satellites with a spatial resolution and geolocation accuracy similar to that of *Meteosat-8* HRV and with a longitudinal separation of at least 50° become available.

After a description of the data, methods, and error sources, the cloud-top height and motion results for the four target areas of different cloud types from June 2004 are discussed.

2. Data

a. Meteosat First Generation

Meteosat First Generation (MFG) is a series of spin-stabilized satellites that rotate at 100 revolutions per minute (i.e., 0.6 seconds per line). The main payload of MFG is the Meteosat Visible and Infrared Imager (MVIRI), which is a three-channel radiometer with channels in the visible (VIS; 0.4–1.1 μm), water vapor (WV; 5.7–7.1 μm), and IR (10.5–12.5 μm) part of the spectrum. The VIS image consists of 5000 × 5000 pixels with 2.25-km resolution at the SSP, and a WV/IR image contains 2500 × 2500 pixels with 4.5-km resolution at the SSP. MVIRI scans the Earth disk from south to north in 25 min. Each scan is followed by a retrace of

the scan mirror and a short period to stabilize the instrument, such that a full disk image is available every 30 min. The operational geolocation for each pixel is accurate to about 1–2 VIS pixels, that is, 2.25–4.5 km at the SSP.

In this study, observations by MVIRI on *Meteosat-5* and -7 were used, with a nominal SSP of 63°E and 0° longitude, respectively. The rectified images obtained from the EUMETSAT archive included the necessary information about the actual satellite position (at image start and image end). For the stereo CTH retrieval, accurate knowledge of the observation geometry and acquisition time of each cloud point to be used in the CTH calculations is required. The observation geometry is thereby given by the satellite position at the acquisition time and the apparent cloud location in each image (i.e., on the reference ellipsoid). For the current study, an updated method to calculate the acquisition for each *Meteosat-5* and -7 pixel was used. In previous work, only the acquisition time for the nominal start and end of the image collection was provided, and a simple linear interpolation method was then used to calculate the acquisition time for each pixel. Detailed information of the acquisition time for each observed image line is now available with this latest implementation of the operational MFG software. The accuracy of the calculated acquisitions for each pixel using the new information is about ±10 s (C. Hanson 2006, personal communication), which is an acceptable accuracy given the slowly changing satellite position. For *Meteosat-5*, differences of up to 30 s were found between the old and new methods to calculate the acquisition time and were mainly due to the satellite's large inclination and the deviations of the SSP from its nominal position. The actual SSP is only provided at image start and end. The satellite position for a specific pixel was approximated by linear interpolation between the satellite positions at image start and image end, using the retrieved approximate acquisition time.

Scanning by *Meteosat-5* and -7 is nearly synchronized, such that, in the overlap region, the time difference between the observations of the two instruments is small. Figure 1 shows the acquisition-time differences between the *Meteosat-5* and -7 observations (calculated with the nominal satellite parameters). The acquisition-time differences are smaller than 10 s for large parts of the overlap region and only increase to 50 s toward the edges of the overlap region. The actual differences can be different from the values shown in Fig. 1, depending on the actual start time of the two images and on the current SSP positions and inclinations of the two satellites.

b. Meteosat Second Generation

Meteosat Second Generation (MSG) succeeded the MFG in 2002. MSG is also spin stabilized and rotates at 100 revolutions per minute. *Meteosat-8*, the first one of this series, is currently located at 3.3°W longitude. SEVIRI is the main payload (Schmetz et al. 2002). Its images are rectified to 0° longitude. SEVIRI has 11 spectral channels with a sampling distance of 3.0 km and one channel (HRV) with a sampling distance of 1.0 km at the SSP. The current absolute *Meteosat-8* HRV geolocation is accurate to about 1.0–2.0 HRV pixels, that is, 1.0–2.0 km at the SSP, which is within the mission requirements of ≤3.0-km absolute geometric accuracy for all 12 channels.

The SEVIRI HRV channel covers only part of the hemisphere to reduce the data size that results from the 3-times-better spatial resolution of this channel versus the other channels; the image consists of an upper and lower segment, which can be shifted to the region of interest(s). For instance, Fig. 2 shows the upper segment centered over Europe and the lower segment shifted to the eastern edge. This configuration is optimal for our stereo CTH retrieval purpose, because it presents a nearly maximal overlap with *Meteosat-5* (except for the upper-right corner in the upper segment).

The raw *Meteosat-8* image contains the mean acquisition time for each image line. With the current small inclination of *Meteosat-8* of nearly zero, the acquisition time for each pixel within the rectified image can be set to the mean acquisition time of the raw line. This approximation is currently accurate to better than 1 s but might get worse if the *Meteosat-8* inclination would significantly increase in the future. The satellite position for a specific pixel was calculated from the given orbit model, using the pixel acquisition time.

Like MVIRI, SEVIRI scans in the south–north direction; however, it uses a different repeat cycle of 15 min (12.5 min for image acquisition and 2.5 min for retrace and stabilization). In Fig. 3, the nominal time difference between *Meteosat-8* and *Meteosat-5* observations is presented. It shows that, because of the different repeat cycles, the largest differences of 450 s are found in the center of the overlap region and they decrease toward the South and North Poles. The values are much larger than those between *Meteosat-5* and *Meteosat-7* (shown in Fig. 1).

c. MISR

The MISR was launched on the *Terra* spacecraft in December of 1999 (Diner et al. 1998). The orbit is sun synchronous at a mean height of 705 km, with an inclination of 98.5° and an equatorial crossing time at about
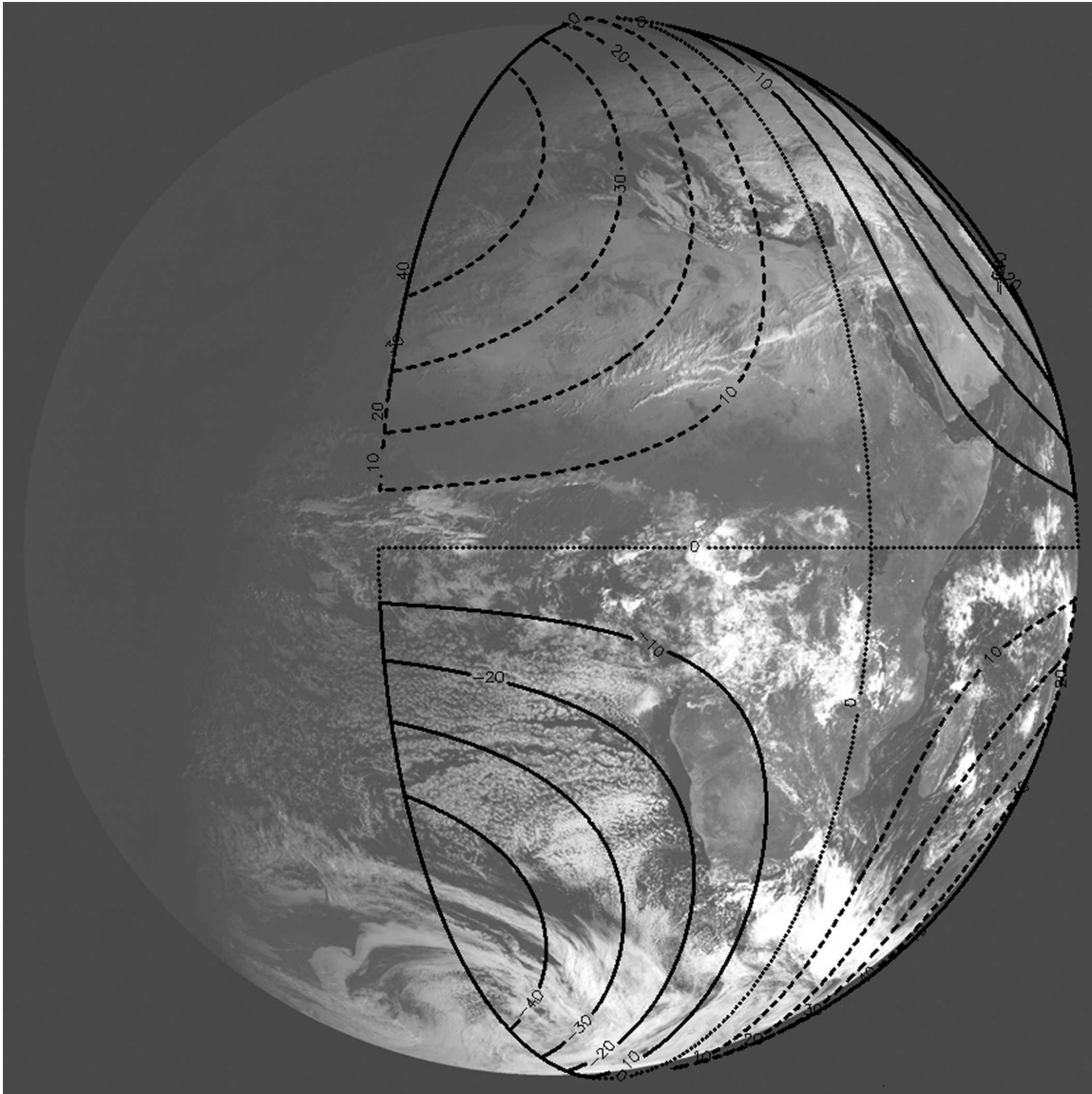
FIG. 1. Acquisition-time difference of M*eteosat-7* and *Meteosat-5* images, ranging from −50 to 50 s.

1030 LT. The repeat cycle is 16 days. The MISR instrument consists of nine push-broom cameras at different viewing angles: −70.5° (named Da), −60.0° (Ca), −45.6° (Ba), −26.1° (Aa), 0.0° (An), 26.1° (Af), 45.6° (Bf), 60.0° (Cf), and 70.5° (Df). The time delay between adjacent camera views is 45–60 s, which results in a total delay between the Da and Df images of about 7 min. The four MISR spectral bands are centered at 446 (blue), 558 (green), 672 (red), and 866 nm [near IR (NIR)]. The data of the red band from all nine cameras and of the blue, green, and NIR bands of the An camera are saved in high resolution, with a pixel size of 275 m × 275 m; the data of the blue, green, and NIR bands of the remaining eight cameras are stored in low reso-

lution, with a pixel size of 1.1 km × 1.1 km. For MISR, the geometric accuracy is high, with an absolute geolocation of all views of 0.5–1.0 pixels, that is, 140–275 m (Jovanovic et al. 2002). In addition, detailed information about the satellite position and the exact acquisition time of each pixel is available.

The operational data products from the National Aeronautics and Space Administration (NASA) are described in the data-products specification documents (MISR 2006); the two products used for our investigations are the "L1B2" ellipsoid data (geolocated product) and the "L2TC" data (top-of-the-atmosphere/cloud product) (Diner et al. 1999; Horváth and Davies 2001; Horváth et al. 2002; Moroney et al. 2002).
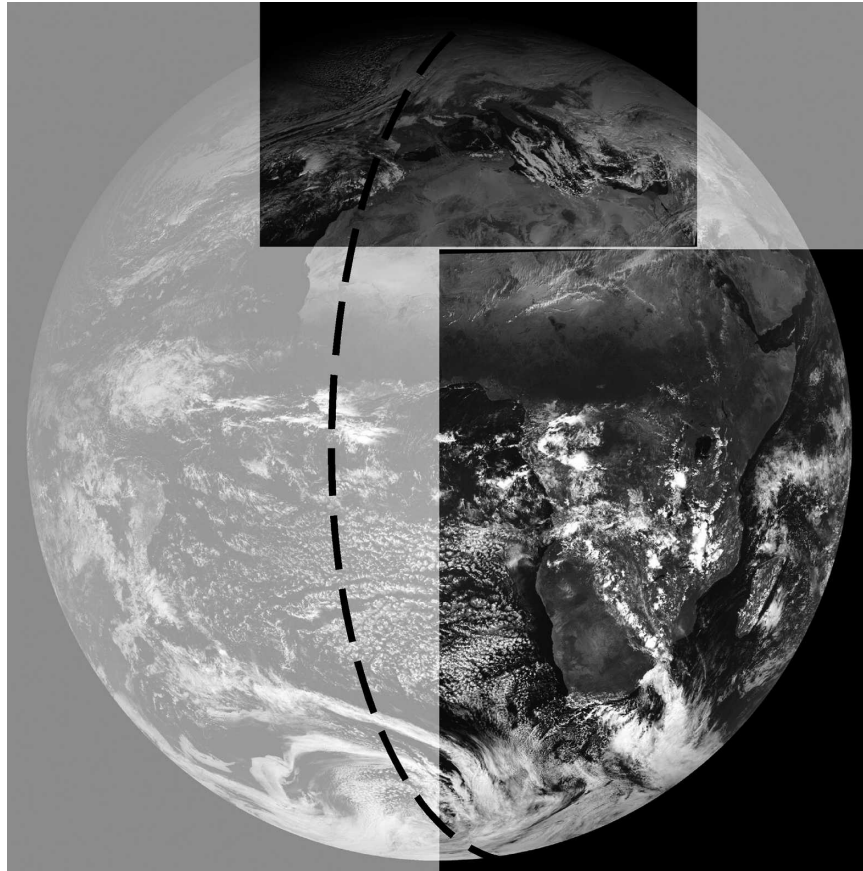
FIG. 2. Upper and lower *Meteosat-8* HRV segments, overlaid on the low-resolution visible channel. The thick dashed line indicates the overlapping area with *Meteosat-5*.

3. Cloud-top height from stereo observations

In the following, the method to derive CTH from stereo observations is briefly described; a complete description of the methods can be found in Seiz (2003). The processing starts with projection of the observations onto a common grid, followed by the selection of the targets for the matching process and a quality-control step.

a. Remapping to common grid

For the matching, all of the images (Meteosat or MISR) should be remapped to a common projection to avoid matching errors that result from distortions. In principle, any target grid and projection can be chosen. Once a common grid is chosen, the remapping is obtained by back projection; that is, each target pixel is back projected into the original image. The value for the target pixel can be calculated using standard interpolation techniques (e.g., cubic, bilinear or nearest neighbor).

For the current analysis, remapping of the observations to either the *Meteosat-5* or *Meteosat-8* HRV projection (i.e., normalized geostationary projection) is not optimal, because these projections are highly distorted toward the image borders. To allow an optimal comparison with the MISR reference data, the Meteosat data were remapped to the MISR space oblique Mercator (SOM) grid of a specific MISR path. For the whole analysis, all images were remapped with cubic interpolation. For the remapping of the Meteosat observations it would have been beneficial to use the original, unrectified observations to avoid loss of precision resulting from multiple resampling. However, the Meteosat data obtained for this study were already rectified to the nominal satellite positions, that is, 0° for *Meteosat-7* and *-8* and 63°E for *Meteosat-5*. Because nearest-neighbor resampling had been applied in the operational EUMETSAT rectification for *Meteosat-5* and *-7*, it resulted in reduced-quality images after the second resampling—in particular, in areas toward the image borders—that negatively influenced the subse-
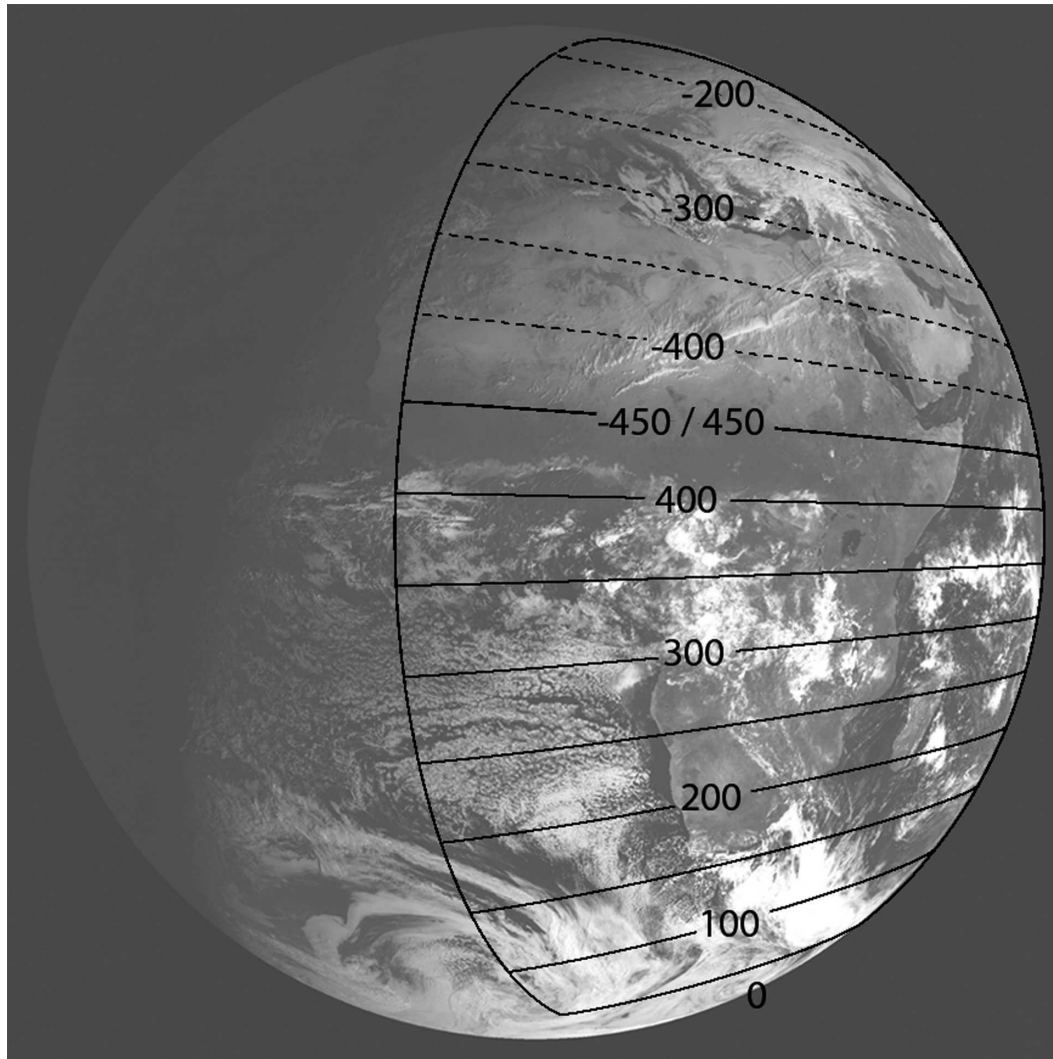
FIG. 3. Acquisition-time difference of *Meteosat-8* and *Meteosat-5* images, ranging between −450 and 450 s. It considers the *Meteosat-8* images at both time *t* and time *t*+1.

quent matching. For future case studies, the optimal operational resampling settings (e.g., cubic convolution) have to be ensured.

b. Matching

The main task of stereo CTH retrieval is the automatic identification of the same cloud features in the multiple views, the so-called matching. Matching of near-simultaneous views from a multiview polar-orbiting instrument (e.g., MISR) and matching/tracking of geostationary images (≤15-min time interval) can be treated with a similar processing chain. A simple flowchart of this matching process is shown in Fig. 4 and consists of a preprocessing step [image enhancement using a Wallis filter (Baltsavias 1991)] followed by the

actual matching and quality control. The multiphoto geometrically constrained (MPGC) matching algorithm developed by Baltsavias (1991), based on least squares matching (LSM) developed by Grün (1985) was adopted, as described in Seiz (2003).

For the MPGC algorithm, three pyramid levels were applied, because no a priori values of the cloud heights were given to the matching algorithm. Pyramid levels represent reduced-resolution images of the original image. Pyramid level 0 indicates the original image, and pyramid levels 1, 2, and 3 are subsequently reduced by a factor of 2 (i.e., 25% of the original image area). Points with good texture were then selected with the Förstner interest operator (Förstner and Gülch 1987). After the MPGC matching, the matching solutions
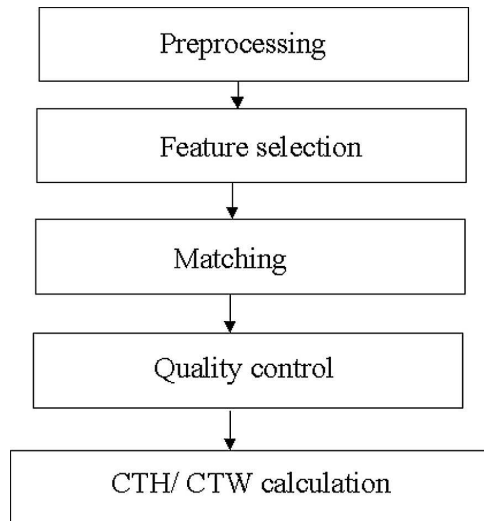
FIG. 4. Overview of the processing steps for multiview CTH/CTW retrieval.

were quality controlled with absolute and relative tests on the matching statistics. The preliminary cloud-top heights were then calculated by intersection of the two viewing rays (see Fig. 5). For the *Meteosat-5/Meteosat-7* combination, it is a near-simultaneous two-view matching so that cloud displacements between the observations are negligible and there is no need to correct the preliminary height for cloud displacements. This is not true for the *Meteosat-5/Meteosat-8* HRV pair and for the CTH derived from MISR observations. Because of the large time differences between the views, changes in the cloud structure can be observed (see Fig. 6). In both cases, the preliminary heights were corrected for the advection error introduced by the cloud motion between the observations as described in Seiz (2003). The applied cloud-motion values were extracted from a sequence of *Meteosat-8* HRV observations using the same matching algorithm. It is important to note that within
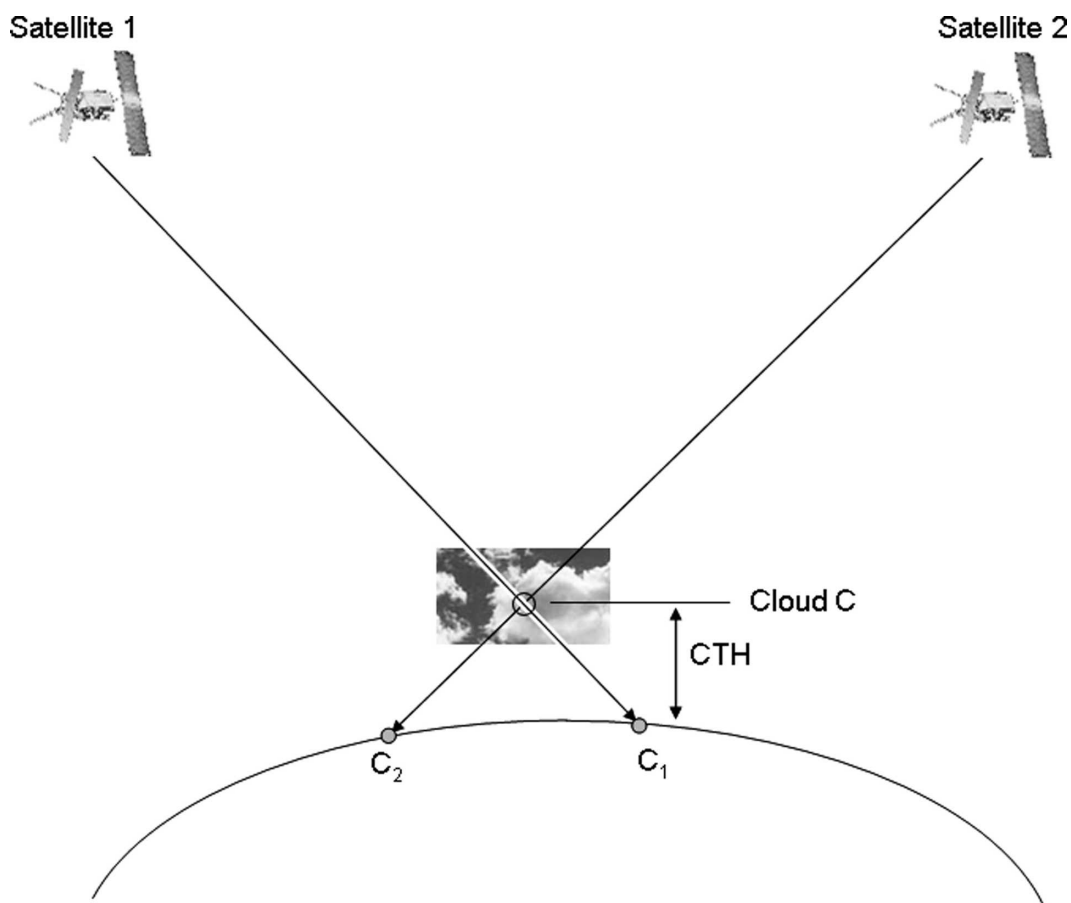

FIG. 5. Illustration of the stereo retrieval geometry, with the cloud target at position C, the two satellite positions, and the observation vectors that define the projection of the cloud target on the earth's surface at C_1 and C_2, respectively. Because of the uncertainties in the satellite position and rectification, the two observation vectors do not intersect at a single point, but cross each other at a certain distance. The minimum distance of the two skew observation vectors defines the CTH for the target C.

```
template              patch_1              patch_2
m8_0630_misr_p156.tif  m8_0645_misr_p156.tif  m5_0630_misr_p156.tif
```


FIG. 6. MPGC triplet matching between (left) *Meteosat-8* HRV at time *t*, (middle) *Meteosat-8* HRV at time *t* + 15 min, and (right) *Meteosat-5*. The template and patch windows are shown as gray squares. It can be seen that there are larger differences in the cloud structures between *Meteosat-8* HRV at time (left) *t* and at (middle) *t* + 15 min, resulting from changes within the 15-min time interval.

the Meteosat stereo retrieval (similar to the MISR retrieval), the CTH and cloud-top winds (CTW) within the 15-min interval were assumed to be constant, with no vertical cloud motion component.

c. Error analysis

The accuracy of the retrieved CTH and CTW with stereo photogrammetric methods is limited by the given geometric configuration (base-to-height[2] ratio B/H; time difference Δt) and by the matching accuracy. Furthermore, the retrieval accuracy can be largely distorted by errors in the geolocation, the satellite position, or the time information. The MPGC LSM matching algorithm generally has high accuracy and reliability—for example, for well-defined points, accuracies of 0.1–0.2 pixels were achieved in laboratory conditions (Baltsavias 1991). However, in the case of clouds, the average accuracy of the matching is only about ±0.5 pixels (Seiz 2003). Table 1 summarizes the estimated accuracies of stereo cloud-top height and motion from *Meteosat-5/-7*, *Meteosat-5/-8* HRV, and MISR for the area of the case study (i.e., 17.5°N, 37.5°E). The preliminary CTH accuracy assumes that the two views have been acquired simultaneously, that is, there was no cloud motion, and is therefore only dependent on the geometric configuration and on the matching accuracy:

$$\sigma_{\text{CTH\_prelim}} = \frac{\Delta_{\text{matching}}}{(B/H)}, \tag{1}$$

with the matching accuracy Δ_{matching} (m) and the base-to-height ratio B/H. For the MPGC LSM matching, we have assumed a matching accuracy of ±0.5 pixels, as described above. A pixel size of 275 m was taken for MISR and an average pixel size was assumed from the *x* dimension (i.e., east–west dimension) of the two Meteosat images, that is, 3.05 km for *Meteosat-5/-7* and 2.1 km for *Meteosat-5/-8* HRV. It is important to note that these theoretical accuracies only include the geometric configuration and the matching accuracy. Systematic errors that could occur (e.g., geolocation errors, satellite-position errors, and/or time errors) are not included in the calculations. The characteristics of the geolocation, satellite-position, and acquisition-time errors have been described in the data description of each sensor in section 2.

Because the same cloud point is not observed simultaneously by the different views or satellites, an additional correction for the cloud advection during the time delay has to be included. The accuracy of this height correction σ_{CTW} is calculated as

$$\sigma_{\text{CTW}} = \frac{\sigma_{v'}\Delta t}{(B/H)}, \tag{2}$$

with the along-track cloud motion accuracy $\sigma_{v'}$ and the time difference Δt. The final CTH accuracy is then calculated from the preliminary CTH accuracy $\sigma_{\text{CTH\_prelim}}$ and the accuracy of the cloud-advection correction σ_{CTW} as

$$\sigma_{\text{CTH\_final}} = (\sigma^2_{\text{CTH\_prelim}} + \sigma^2_{\text{CTW}})^{1/2}. \tag{3}$$

Another error source, which has also to be considered in this analysis, is the validity of the assumptions. As

---

[2] The base *B* is defined as the distance of the two satellite positions, projected on the earth's surface; the height *H* is the altitude of the satellite.

TABLE 1. Theoretical accuracies of the stereo CTH as derived from *Meteosat-5/-7* and *Meteosat-5/Meteosat-8* HRV stereo pairs, of the operational MISR L2TC product, and as derived from MISR L1B2 An–Aa observations using the *Meteosat-8*-derived cloud displacements. In addition, the potential future *Meteosat-8/-9* HRV combination is listed. For MISR L1B2 An–Aa and Meteosat, the values are calculated assuming a measurement accuracy of ±0.5 pixels, with an average pixel size of 3.05 km for the *Meteosat-5/-7* (M5 and M7) combination and 2.1 km for the *Meteosat-5/-8* HRV (M5 and M8) combination, respectively. For the *Meteosat-8/-9* HRV combination, the location of the two MSG satellites is assumed to be at 3.3°W and 63°E. For MISR L2TC, the accuracy estimates given by Horváth and Davies (2001) and Moroney et al. (2002) are used. The Meteosat theoretical accuracies are calculated for the region of interest (i.e., 17.5°N, 37.5°E) only, whereas the MISR estimates are valid for the whole path.

Sensor	Pixel size (km)	B/H	Δt (s)	Preliminary CTH accuracy (σ_{CTH}) (m)	Cloud-motion accuracy ($\sigma_{v'}$) (m s^{-1})	Final CTH accuracy (m)
Meteosat-5/-7	2.7 × 2.4 (M5)	1.5	—	1020	—	1020
	3.4 × 2.4 (M7)		(<10)			
Meteosat-5/-8 HRV	2.7 × 2.4 (M5)	1.7	390	620	2.0	1000
	1.5 × 1.1 (M8)				(from M8)	
Meteosat-8/-9 HRV	1.5 × 1.1	1.7	—	440	—	440
Operational MISR L2TC product	0.275	0.49	46	560	3.0 (from MISR triplet)	630
MISR L1B2 An–Aa	0.275	0.49	46	280	2.0 (from M8)	340

described above, it is assumed that the CTH and CTW within the 15-min interval are constant, with no vertical cloud-motion component. So, stereo CTH errors can likely occur in regions with strong vertical cloud motion. Furthermore, the area-based MPGC LSM assumes a locally smooth surface, which is of course not always fulfilled within clouds, especially at cloud layer discontinuities or at cloud borders.

4. Results

Stereo height retrieval from geostationary satellite observations was tested within four target areas (13°–22°N, 36°–39°E) at about 0815 UTC 5 June 2004. Four different cloud fields were selected for the analysis based on a number of criteria. The main two criteria were the proximity to coastlines, because these were needed to check the georectification of the Meteosat images, and the availability of coincident MISR observations. Furthermore, the clouds were selected to represent different cloud surface properties and geometrical shape. No attempt was made to select a wide variety of suitable targets because the objective was not to perform a comprehensive study. Instead, the objective was to perform a pilot study to document the applicability of stereo methods for CTH determination from the European geostationary satellites. The four cloud targets are shown in Fig. 7; the detailed acquisition times are listed in Table 2.

In Table 3, the matching statistics of the four cloud areas are listed. More cloud points in the *Meteosat-5/-8* HRV triplet matching failed (e.g., because of disappearance of cloud structures or appearance of new features within the 15-min time interval) or were rejected

in the quality control than for the *Meteosat-5/-7* combination. The time difference of nearly 7.5 min between the *Meteosat-8* HRV and *Meteosat-5* images seems to have a considerable influence on the matching success rate and accuracy in comparison with the near-simultaneous *Meteosat-5/-7* matching.

The stereo CTH derived from Meteosat for these cloud areas are summarized in Table 4. The table shows the mean CTH for all successfully matched targets within the cloud field and its standard deviation. From these results, it can be seen that the CTHs derived from the *Meteosat-5/-7* pair are consistently larger by about 2.5 km than the results from the *Meteosat-5/-8* HRV pair. From the low standard deviations, we can conclude that the matching results from the successfully matched targets are consistent. The *Meteosat-5/-8* HRV standard deviations are larger than those for *Meteosat-5/-7*, which can probably be attributed to the increased matching difficulties arising from the large time difference.

A measure for the geometric consistency of the CTH solution is the value of the minimum intersection distance between the two rays. The geolocation accuracy has an enormous effect on the minimum intersection distance. For the minimum distance, parallax errors in dx and dy are both equally important; for CTH, mainly parallax errors in dx are critical. The values of the minimum intersection distance shown in Table 4 are relatively large in comparison with the expected CTH accuracy. Values up to 3 km for *Meteosat-5/-7* and up to 2.5 km for *Meteosat-5/-8* HRV are calculated, which could translate into a CTH error of up to a few kilometers. These results indicate that the accuracy of the Meteosat geolocation is not optimal.
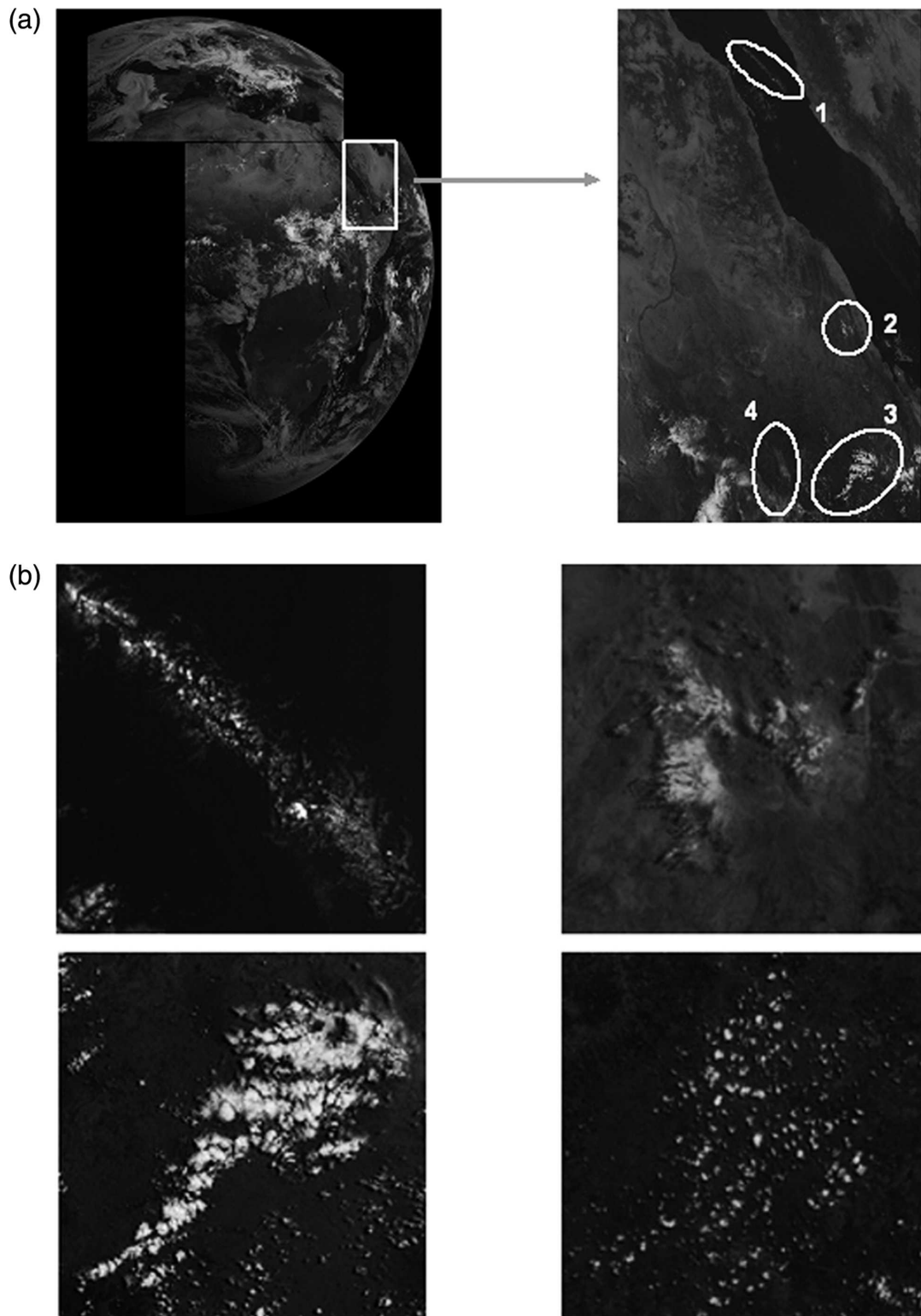
FIG. 7. Cloud target areas in the region of 13°–22°N, 36°–39°E: (a) overview of cloud areas and (b) zoom of the cloud areas in the *Meteosat-8* HRV image of 0800 UTC [in (b), shown are (top left) cloud 1, (top right) cloud 2, (bottom left) cloud 3, and (bottom right) cloud 4].

TABLE 2. Acquisition times (UTC) of *Meteosat-5*, *Meteosat-7*, and *Meteosat-8* HRV, MISR, and MODIS on 5 Jun 2004.

Scene	Meteosat-5 (m5_0800)	Meteosat-7 (m7_0800)	Meteosat-8 (m8_0800)	Meteosat-8 (m8_0815)	MISR (and MODIS)
5 Jun 2004, 17.5°N, 37.5°E (MISR path 170, block 76)	0816:38	0816:33	0808:08	0823:07	AN: 0807:32

To demonstrate this assumption, the relative geolocation accuracy of each remapped Meteosat image was determined versus the MISR nadir image (i.e., An) with about 50 points along the coastlines of the Red Sea. The coastline points were matched automatically with MPGC LSM matching, using the second pyramid level of the MISR An image. The measured relative geolocation shifts are listed in Table 5, showing that the current geolocation accuracy of *Meteosat-8* HRV is only of the same order as the MFG geolocation accuracy. Therefore, it appears as if there are still systematic errors in the operational *Meteosat-8* HRV geolocation that should be eliminated if possible. On the contrary, the measurement *accuracy* of the coastline points is unexpectedly high—in particular, for the *Meteosat-8* HRV images, with standard deviations of less than 0.2 MISR SOM pixels, that is, less than 220 m, in both *dx* and *dy*. Thus, the operational geolocation of Meteosat images can be fine-corrected locally with well-defined coastlines with an accuracy of about 200–300 m for MFG images and less than 200 m for *Meteosat-8* HRV images.

Table 6 show the stereo CTH from the geostationary satellite observations after the geolocation correction. The results show that the corrections are larger for the *Meteosat-5/-7* combination; the corrected *Meteosat-5/-7* CTH results are now lower than the uncorrected ones. The reverse is true for the *Meteosat-5/-8* HRV CTH results. Because the relative geolocation correction between *Meteosat-5* and *Meteosat-8* HRV is mainly in *dy*, the influence of the geolocation correction on the absolute CTH is less for the *Meteosat-5/-8* HRV than for the *Meteosat-5/-7* combination. A consequence of the

geolocation correction is that the CTH results are now consistent between the two Meteosat stereo combinations. The corrections also resulted in a significant reduction of the minimal intersection distance, which increases the confidence in the results.

The remarks above describe the matching and geolocation effects, but it is important to compare the final Meteosat stereo cloud-top heights with other available CTH products. In Table 7, the corresponding CTH values from the operational MISR L2TC and the MODIS "MOD06" products are listed. Table 8 summarizes the CTW results for the four cloud target areas. The MODIS cloud-top pressure (CTP) values were converted into CTH with a nearby sounding (OEJN Jeddah, 41024, 21.7°N, 39.18°E). Details about the operational MISR L2TC stereo CTH product can be found in Diner et al. (1999), Horváth and Davies (2001), Moroney et al. (2002), and Muller et al. (2002), and the MODIS MOD06 algorithms are described in Menzel et al. (2002). In addition to these operational products, our stereo CTH retrieval method from the geostationary satellite observations was applied to the MISR observations using the An and Aa cameras. For the correction of the MISR An–Aa preliminary CTHs, the cloud-top wind values extracted from *Meteosat-8* HRV were used. Figure 8 summarizes the findings in a scatterplot, where the operational MISR CTHs have been taken as reference.

The results of this limited study indicate that, except for the value for cloud 1, all stereo CTHs, after applying the geolocation correction, are within the theoretical Meteosat error estimates of 1000 m (see Table 1) from the MISR results. There is a suggestion that there might be two cloud layers, to which the MISR and Meteosat

TABLE 3. Matching statistics of the two Meteosat stereo combinations. The total number of targets within each cloud field, the number of targets for which the matching was successful, and the number of targets after the quality control (QC) are listed.

	Meteosat-5/-7 No. of targets			Meteosat-5/-8 HRV No. of targets		
	Total	Matched	After QC	Total	Matched	After QC
Cloud 1	72	71	62	72	62	43
Cloud 2	41	41	32	41	41	37
Cloud 3	68	67	61	68	67	42
Cloud 4	49	49	47	49	46	39

TABLE 4. Mean stereo CTHs and standard deviations for the four cloud targets derived from the two Meteosat stereo combinations, *before* the geolocation correction. Also shown in the table are the mean minimal distances (dist) of the forward intersections.

	Meteosat-5/-7		Meteosat-5/-8 HRV	
	CTH (m)	Dist (m)	CTH (m)	Dist (m)
Cloud 1	9301 ± 274	2882	7104 ± 249	2235
Cloud 2	8846 ± 177	2286	6243 ± 245	2380
Cloud 3	8128 ± 214	2852	5596 ± 312	1958
Cloud 4	4501 ± 274	2916	1908 ± 456	2084

TABLE 5. Geolocation correction for *Meteosat-5*, *-7*, and *-8* HRV vs MISR An (in MISR SOM pixels; i.e., 1 pixel = 1100 m) in east–west (*dx*) and north–south (*dy*) direction, 5 Jun 2004, MISR path 170, blocks 71–81.

Sensor	dx	dy
Meteosat-5, 0800 UTC	-2.10 ± 0.13	-3.54 ± 0.20
Meteosat-7, 0800 UTC	0.39 ± 0.18	-0.94 ± 0.28
Meteosat-8, 0800 UTC	-2.74 ± 0.09	-1.38 ± 0.18
Meteosat-8, 0815 UTC	-3.15 ± 0.11	-1.19 ± 0.10

TABLE 7. CTH results of comparison satellite data, MISR L1B2 An–Aa (with *Meteosat-8* wind correction), MISR L2TC "BestWinds" stereo height product, and MODIS MOD06 cloud-top pressure product (converted into CTH with nearby sounding).

	MISR L1B2 An–Aa CTH, wind_corr (m)	MISR L2TC CTH, best_winds (m)	MODIS MOD06 CTH, converted (m)
Cloud 1	5672 ± 194	6156 ± 146	7883 ± 595
Cloud 2	5931 ± 184	5954 ± 368	8949 ± 1851
Cloud 3	5953 ± 254	6459 ± 400	7512 ± 753
Cloud 4	2680 ± 105	2904 ± 396	975 ± 305

observations are not equally sensitive. For example, both Meteosat combinations indicate a CTH of about 7300–7800 m for cloud 1 and a CTH of about 6800–7000 m for cloud 2, respectively. For both clouds, the MISR results indicate a much smaller value of approximately 6000 m. The very high MODIS CTHs for these two clouds are a further indication for a possible multilayer cloud situation. Results from Meteosat for clouds 3 and 4 agree very well with the operational MISR CTHs.

We have applied the same method as used for the geostationary stereo retrieval to the MISR L1B2 An–Aa observations, including the correction for cloud displacement between the two MISR observations using cloud winds derived from *Meteosat-8* HRV. The results from this ("MISR LSM") confirmed the operational MISR L2TC results. In Table 7, we see that both the operational (i.e., L2TC) and the MISR LSM results agree very well but clearly show the effect of the different CTW values used in the correction (Table 8). The accuracy for these four cloud areas is about 200–300 m for MISR LSM and 200–400 m for MISR L2TC, and so they are well suited for validation of other height products.

Last, the derived CTHs are compared with the MODIS values. These were calculated from the operational MODIS MOD06 CTP product using the sounding station located near the Red Sea (OEJN Jeddah, 41024, 21.7°N, 39.18°E; 1200 UTC sounding). Figure 8 and Table 7 indicate that for cloud 1, the MODIS CTHs appear to be close to the Meteosat results. For clouds 2

and 3, the MODIS CTHs are considerably higher than the stereo CTH results. For cloud 4, the MODIS results are considerably lower than any of the stereo CTH results. It is known that the method to derive CTP from the MODIS observations has its lowest accuracy for low-level clouds (Preusker et al. 2005; Naud et al. 2005b). Also, the conversion from CTP to CTH using the sounding might introduce errors because the sounding location was not in the proximity of cloud 4. In this case especially, the lower part of the atmospheric profile might not be representative, which could explain part of the differences in CTH for cloud 4.

5. Conclusions and outlook

In this paper, the possibilities of stereo cloud-top height retrievals from the currently operational Meteosat satellites have been analyzed. In particular, the new *Meteosat-5/-8* HRV combination has been tested. The geolocation, satellite-position, and acquisition-time characteristics of each Meteosat satellite have been studied. To account for the time difference between the *Meteosat-5* and *Meteosat-8* HRV acquisition, two subsequent *Meteosat-8* HRV images were taken and the cloud-advection effect was corrected by tracking targets between the two. From the results, we can see that the matching accuracy is similar for the *Meteosat-5/-7* and *Meteosat-5/-8* HRV combinations, which is a conse-

TABLE 6. Mean stereo CTHs and standard deviations for the four cloud targets derived from the two Meteosat stereo combinations, *after* the geolocation correction. Also shown in the table are the mean minimal distances (dist) of the forward intersections.

	Meteosat-5/-7		*Meteosat-5/-8*	
	CTH (m)	Dist (m)	CTH (m)	Dist (m)
Cloud 1	7341 ± 274	182	7802 ± 249	242
Cloud 2	6858 ± 177	716	6982 ± 245	277
Cloud 3	6129 ± 215	218	6361 ± 311	404
Cloud 4	2491 ± 274	233	2685 ± 457	482

TABLE 8. CTW results from *Meteosat-8* and MISR L2TC. Positive CTW values are west to east for u' and south to north for v', respectively.

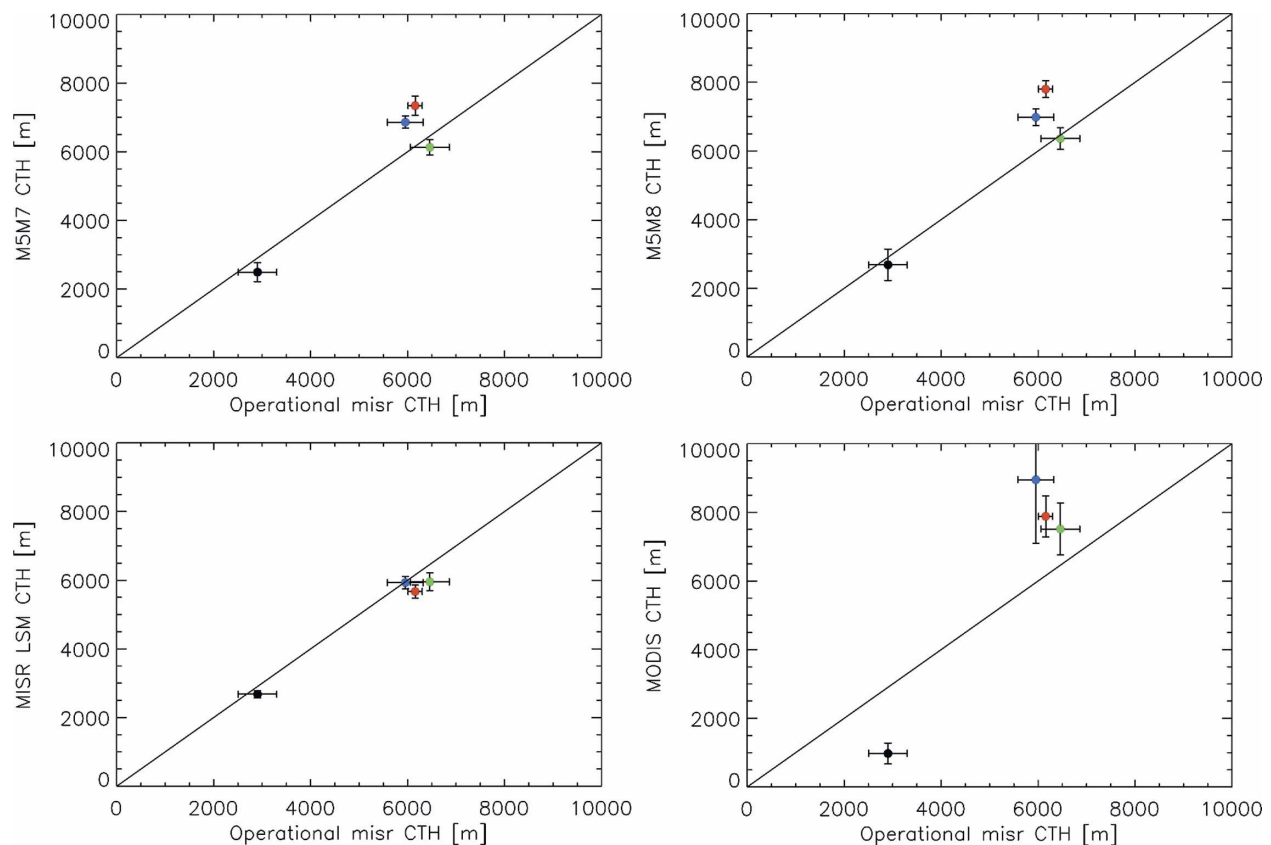|	Cross-track wind u' *Meteosat-8* (m s^{-1})	Along-track wind v' *Meteosat-8* (m s^{-1})	Cross-track wind u' MISR L2TC (m s^{-1})	Along-track wind v' MISR L2TC (m s^{-1})
Cloud 1	-2.9 ± 1.9	7.4 ± 2.8	-2.9 ± 1.3	1.0 ± 0.3
Cloud 2	0.0 ± 1.0	-1.2 ± 1.6	-1.2 ± 0.1	-2.1 ± 2.2
Cloud 3	-5.8 ± 1.4	-0.6 ± 1.5	-8.4 ± 1.0	-4.2 ± 2.4
Cloud 4	2.8 ± 1.7	0.5 ± 1.3	0.9 ± 1.1	-1.4 ± 4.2

FIG. 8. Scatterplots of the CTH derived from the study for the two Meteosat stereo combinations, the MISR LSM retrieval, and the operational MODIS retrieval. As reference, the operational MISR L2TC CTH results were taken. Red indicates cloud 1, blue is cloud 2, green is cloud 3, and black is cloud 4.

quence of the higher spatial resolution of *Meteosat-8* HRV versus the better time synchronization of the *Meteosat-5/-7* combination. Furthermore, the results have shown that the accuracy of the geostationary CTH retrieval can be improved substantially for areas near coastlines by applying a geolocation correction derived from coastline points, using, for example, the accurately geolocated MISR An image as reference. The effect of this geolocation correction was confirmed by a large decrease of the minimum intersection distance in the forward intersections for both Meteosat stereo combinations. With the geolocation correction, as well as the newly implemented time information in the *Meteosat-5* and *-7* header information, the stereo cloud-top height assignment for the *Meteosat-5/-7* and *Meteosat-5/-8* HRV combinations resulted in about the same accuracy of approximately ±1 km. For the *Meteosat-5/-8* HRV combination, the large time differences of up to 7.5 min are preventing an even higher accuracy.

Quantitative comparisons of the *Meteosat-5/-7* and *Meteosat-5/-8* HRV stereo heights have been performed with MISR LSM, MISR L2TC, and MODIS

CTHs for four different cloud areas. In three of the four cloud cases examined, the Meteosat and MISR CTHs agree to within their expected errors. In only one case, the difference exceeds the expected error, with Meteosat indicating a higher cloud. For the mid-/high-level cloud cases, the corresponding MODIS CTHs were consistently higher than those of Meteosat and MISR. The disagreement with MODIS is not yet understood. It could be that thin layers of high cirrus are affecting the MODIS results but are not observed well by the Meteosat and MISR visible channels. Further investigation using the infrared channels of *Meteosat-8*, especially the 6.3-μm channel, may help to resolve this issue.

In conclusion, further stereo CTH retrieval tests with Meteosat satellites should include a geolocation correction strategy and a scanning configuration with smaller time differences (e.g., two synchronized MSG satellites with an adequate longitudinal separation). A further improvement of the geolocation and, eventually, quality of the images could be achieved by starting with the raw images and applying the EUMETSAT sensor model with additional ground-control and tie points or

even using an own sensor model for local image recti-fication. The Meteosat stereo heights would then rep-resent a good independent validation method for the operational Meteosat height assignment techniques.

REFERENCES

Baltsavias, E. P., 1991: Multiphoto geometrically constrained matching. Ph.D. dissertation, Institute of Geodesy and Pho-togrammetry, ETH Zurich, Mitteilungen 49, 221 pp.

Campbell, G., and K. Holmlund, 2000: Geometric cloud heights from Meteosat and AVHRR. *Proc. Fifth Int. Winds Work-shop,* Publication EUM P28, Lorne, Australia, EUMETSAT, 109–115.

——, and ——, 2004: Geometric cloud heights from Meteosat. *Int. J. Remote Sens.,* **25,** 4505–4519.

Diner, D., and Coauthors, 1998: Multi-angle Imaging SpectroRa-diometer (MISR) description and experiment overview. *IEEE Trans. Geosci. Remote Sens.,* **36,** 1072–1087.

——, and Coauthors, 1999: MISR level 2 cloud detection and classification. JPL Tech. Rep. ATBD-MISR-07, 102 pp.

Förstner, W., and E. Gülch, 1987: A fast operator for detection and precise location of distinct points, corners, and centers of circular features. *Proc. ISPRS Intercommission Conf. on Fast Processing of Photogrammetric Data,* Interlaken, Switzer-land, ISPRS, 281–305.

Fujita, T., 1982: Principle of stereoscopic height computations and their applications to strato-spheric cirrus over severe thun-derstorms. *J. Meteor. Soc. Japan,* **60,** 355–368.

Grün, A., 1985: Adaptive least squares correlation: A powerful image matching technique. *South Afr. J. Photogramm. Re-mote Sens. Cartogr.,* **14,** 175–187.

Hasler, F., 1981: Stereographic observations from geosynchronous satellites: An important new tool for the atmospheric sci-ences. *Bull. Amer. Meteor. Soc.,* **62,** 194–212.

Horváth, A., and R. Davies, 2001: Feasibility and error analysis of cloud motion wind extraction from near-simultaneous multi-angle MISR measurements. *J. Atmos. Oceanic Technol.,* **18,** 591–608.

——, ——, and G. Seiz, 2002: Status of MISR cloud-motion wind product. *Proc. Sixth Int. Winds Workshop,* Publication EUM P35, Madison, WI, EUMETSAT, 269–275.

Jovanovic, V. M., M. A. Bull, M. M. Smyth, and J. Zong, 2002: MISR in-flight camera geometric model calibration and geo-rectification performance. *IEEE Trans. Geosci. Remote Sens.,* **40,** 1512–1519.

Menzel, P., B. Baum, K. Strabala, and R. Frey, 2002: Cloud top properties and cloud phase algorithm theoretical basis docu-ment. Document ATBD-04, version 7, 56 pp. [Available on-line at http://modis.gsfc.nasa.gov/data/atbd/atbd_mod04.pdf.]

MISR, cited 2006: MISR data products specifications. [Available online at http://eosweb.larc.nasa.gov/PRODOCS/misr/DPS/.]

Moroney, C., R. Davies, and J.-P. Muller, 2002: Operational re-trieval of cloud-top heights using MISR data. *IEEE Trans. Geosci. Remote Sens.,* **40,** 1532–1540.

Muller, J. P., A. Mandanayake, C. Moroney, R. Davies, D. J. Diner, and S. Paradise, 2002: MISR stereoscopic image matchers: Techniques and results. *IEEE Trans. Geosci. Re-mote Sens.,* **40,** 1547–1559.

Naud, C., J.-P. Muller, and P. de Valk, 2005a: On the use of ICESAT-GLAS measurements for MODIS and SEVIRI cloud-top height accuracy assessment. *Geophys. Res. Lett.,* **32,** L19815, doi:10.1029/2005GL023275.

——, ——, E. E. Clothiaux, B. A. Baum, and W. P. Menzel, 2005b: Intercomparison of multiple years of MODIS, MISR and radar cloud-top heights. *Ann. Geophys.,* **23,** 2415–2424.

Nieman, S. A., J. Schmetz, and P. Menzel, 1993: A comparison of several techniques to assign heights to cloud tracers. *J. Appl. Meteor.,* **32,** 1559–1568.

Preusker, R., J. Fischer, G. Seiz, D. Poli, A. Grün, C. Poulsen, and R. Siddans, 2005: Validation of cloud-top pressure derived from MSG-SEVIRI observations through a comparison with independent observations. EUMETSAT Final Rep. Contract EUM/CO/03/R08/SAT, 262 pp. [Available online at http://www.eumetsat.int/Home/Main/Publications/Technical_and_Scientific_Documentation/Technical_Memoranda/SP_1124282681564?l=en.]

Schmetz, J., P. Pili, S. Tjemkes, D. Just, J. Kerkmann, S. Rota, and A. Ratier, 2002: An introduction to Meteosat Second Gen-eration (MSG). *Bull. Amer. Meteor. Soc.,* **83,** 977–992.

Seiz, G., 2003: Ground- and satellite-based multi-view photogram-metric determination of 3D cloud geometry. Ph.D. thesis, ETH Zuerich, IGP Mitteilungen 80, 177 pp.

——, and E. P. Baltsavias, 2000: Satellite- and ground-based ste-reo analysis of clouds during MAP. *Proc. EUMETSAT Us-ers' Conf.,* EUM P29, Bologna, Italy, EUMETSAT, 805–812.

——, ——, and A. Grün, 2001: Comparison of satellite-based cloud-top height and wind from MISR, ATSR2 and *Meteo-sat-6* rapid scans. *Proc. EUMETSAT Users' Conf.,* EUM P33, Antalya, Turkey, EUMETSAT, 224–230.

——, ——, and ——, 2003: High-resolution cloud motion analysis with *Meteosat-6* rapid scans, MISR and ASTER. *Proc. EUMETSAT Meteorological Satellite Conf.,* EUM P39, Wei-mar, Germany, EUMETSAT, 352–358.

Wylie, D. P., D. Santek, and D. Starr, 1998: Cloud-top heights from *GOES-8* and *GOES-9* stereoscopic imagery. *J. Appl. Meteor.,* **37,** 405–413.